ISSN 1027-4510, Journal of Surface Investigation: X-ray, Synchrotron and Neutron Techniques, 2024, Vol. 18, No. 3, pp. 614–619. © Pleiades Publishing, Ltd., 2024.

Transition Radiation on a Conducting Target Shaped as a Right Dihedral Angle

V. V. Syshchenko[a], *, A. I. Tarnovsky[a], and V. A. Krivtsov[a]

[a] *Belgorod State National Research University, Belgorod, 308015 Russia*

**e-mail: syshch@yandex.ru*

Received September 30, 2023; revised November 25, 2023; accepted November 25, 2023

Abstract—The transition radiation of a charged particle in the simplest case of incidence on an infinitely conductive, ideal plane can be described based on the well-known method of images from electrostatics. This method also enables finding the distribution of fields in more complex cases, such as the field of a point particle in the presence of two intersecting conducting planes, the angle between which divides the angle 180° evenly. Based on the method of images, we describe the transition radiation that occurs when a fast charged particle strikes a target consisting of two conducting half-planes intersecting at right angles (from the inside of a dihedral angle). The characteristics of radiation emitted by fast and slow particles are qualitatively examined, and their visual interpretation is given. The possibility of using interference effects arising from radiation for monitoring beams of charged particles is discussed.

Keywords: transition radiation, method of images, particle monitoring, beam diagnostics

DOI: 10.1134/S1027451024700198

INTRODUCTION

Transition radiation occurs when a uniformly moving charged particle crosses the interface between two media with different electromagnetic properties [1–3]. It was predicted for the simplest case of an infinite flat interface between free space and an ideal conductor [4], based on the mirror-image method known from electrostatics (for example, [2, 3]). In this method, the boundary conditions on the metal surface are satisfied by introducing, alongside the charge of the incident particle, its "mirror image" (a fictitious charge). In cases of more complex geometries, the result can be achieved by introducing multiple fictitious charges. For example, diffraction and transition radiation on spherical and semispherical surfaces was described [5–9].

In the present study, the theory of transition radiation on a target in the form of two infinite half-planes intersecting at right angles is developed. A visual interpretation of the angular distribution of the emitted radiation is given on the magnitude and direction of velocity of the incident particle, as well as the coordinates of the point of particle impact on the conductor surface.

Transition radiation is widely used for diagnosing and monitoring beams of charged particles (see, for example, [10–15]). Due to its interference nature, transition radiation at a dihedral angle can also be utilized for these purposes.

EXPERIMENTAL

In the mirror-image method [2, 3], the effect of a conducting surface on the distribution of the electric field in space is simulated by introducing, alongside a real point charge, one or more fictitious charges ("images" of the real charge). In the simplest case of a point charge e and a grounded conducting infinite plane, the distribution of the electric field is the same as that of two point charges (real and fictitious (charge $-e$), positioned symmetrically relative to the plane. In a more complex scenario involving two intersecting conducting half-planes, boundary conditions on the surface of the conductor are satisfied by introducing three fictitious charges (see any textbook on electrodynamics, for example [3]).

Let us consider a situation where a real charge moves rectilinearly and uniformly with velocity $\mathbf{v}_1$ at angle ψ to the normal of one of the two half-planes (Fig. 1), reaching it at time $t = 0$, where the point of collision of the particle with the plane has the coordinate x_0. The resulting radiation can be easily described based on known equations for radiation from an arbitrarily moving point charge (e.g., [16–18]). The amplitude of the diverging wave of the vector potential of the radiation field is proportional to the magnitude

$$\mathbf{I} = e\int_{-\infty}^{\infty}\mathbf{v}(t)\exp\left[i\left(\omega t - \mathbf{kr}(t)\right)\right]dt, \qquad (1)$$

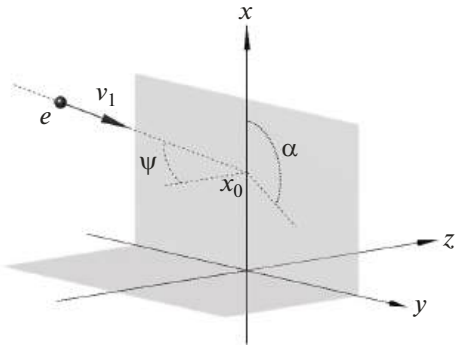

Fig. 1. Incidence of charge e onto a conducting dihedral angle. All dashed lines lie in the same plane.

where ω and $\mathbf{k}$ are the frequency and wave vector of the emitted wave; $|\mathbf{k}| = \omega/c$; c is the speed of light in free space; e, $\mathbf{r}(t)$, and $\mathbf{v}(t)$ are the magnitude, trajectory, and velocity of the charge; and the spectral-angular radiation density is expressed by the equation

$$\frac{dE}{d\omega d\Omega} = \frac{1}{4\pi^2 c}\left|\mathbf{k}\times\mathbf{I}\right|^2. \tag{2}$$

In the case under consideration, vector $\mathbf{I}$ contains four terms, describing four partial contributions from the incident particle and its three images:

$$\begin{aligned}\mathbf{I} &= e\mathbf{v}_1\int_{-\infty}^{0}\exp\left[i\left(\omega t - \mathbf{k}\mathbf{v}_1 t - k_x x_0\right)\right]dt - e\mathbf{v}_2\int_{-\infty}^{0}\exp\left[i\left(\omega t - \mathbf{k}\mathbf{v}_2 t - k_x x_0\right)\right]dt\\ &- e\mathbf{v}_3\int_{-\infty}^{0}\exp\left[i\left(\omega t - \mathbf{k}\mathbf{v}_3 t + k_x x_0\right)\right]dt + e\mathbf{v}_4\int_{-\infty}^{0}\exp\left[i\left(\omega t - \mathbf{k}\mathbf{v}_4 t + k_x x_0\right)\right]dt\\ &= -ie\left\{\frac{\mathbf{v}_1}{\omega - \mathbf{k}\mathbf{v}_1} - \frac{\mathbf{v}_2}{\omega - \mathbf{k}\mathbf{v}_2}\right\}\exp\left(-ik_x x_0\right) + ie\left\{\frac{\mathbf{v}_3}{\omega - \mathbf{k}\mathbf{v}_3} - \frac{\mathbf{v}_4}{\omega - \mathbf{k}\mathbf{v}_4}\right\}\exp\left(ik_x x_0\right),\end{aligned} \tag{3}$$

where the charge velocity components are

$$\begin{aligned}\mathbf{v}_1 &= v\left(\sin\psi\cos\alpha, \sin\psi\sin\alpha, \cos\psi\right),\\ \mathbf{v}_2 &= v\left(\sin\psi\cos\alpha, \sin\psi\sin\alpha, -\cos\psi\right),\\ \mathbf{v}_3 &= v\left(-\sin\psi\cos\alpha, \sin\psi\sin\alpha, \cos\psi\right),\\ \mathbf{v}_4 &= v\left(-\sin\psi\cos\alpha, \sin\psi\sin\alpha, -\cos\psi\right).\end{aligned}$$

The first pair of terms in (3) describes the radiation resulting from the particle's incidence on the infinite plane (x, y), while the second pair describes the reflection of this radiation from the plane (y, z), with differences in the phase factors accounting for the interference between these two contributions. For the convenience of further analysis, we introduce a unit vector in the direction of the wave vector of the emitted wave,

$$\mathbf{e}_k = \frac{\mathbf{k}}{|\mathbf{k}|} = \left(\sin\theta\cos\varphi, \sin\theta\sin\varphi, \cos\theta\right)$$

and rewrite (3) as follows:

$$\mathbf{I} = -\frac{ie}{\omega}\frac{\mathbf{v}_1 - \mathbf{v}_2 - \frac{1}{c}\mathbf{e}_k\times\left(\mathbf{v}_1\times\mathbf{v}_2\right)}{\left(1 - \frac{1}{c}\mathbf{e}_k\mathbf{v}_1\right)\left(1 - \frac{1}{c}\mathbf{e}_k\mathbf{v}_2\right)}\exp\left(-ik_x x_0\right) + \frac{ie}{\omega}\frac{\mathbf{v}_3 - \mathbf{v}_4 - \frac{1}{c}\mathbf{e}_k\times\left(\mathbf{v}_3\times\mathbf{v}_4\right)}{\left(1 - \frac{1}{c}\mathbf{e}_k\mathbf{v}_3\right)\left(1 - \frac{1}{c}\mathbf{e}_k\mathbf{v}_4\right)}\exp\left(ik_x x_0\right). \tag{4}$$

Substituting (4) into (2) and taking into account that

$$\mathbf{v}_1 - \mathbf{v}_2 = \mathbf{v}_3 - \mathbf{v}_4 = 2v\cos\psi\mathbf{e}_z, \tag{5}$$

where $\mathbf{e}_z$ is the unit vector along the z axis, we obtain an expression for the spectral-angular radiation density,

$$\frac{dE}{d\omega d\Omega} = \frac{e^2v^2}{4\pi^2c^3}4\cos^2\psi$$
$$\times\left\{\frac{1-(\mathbf{e}_k\mathbf{e}_z)^2+\frac{V^2}{c^2}\sin^2\psi\left(1-\left(\mathbf{e}_k(\sin\alpha\mathbf{e}_x-\cos\alpha\mathbf{e}_y)\right)^2\right)-2\frac{V}{c}\sin\psi\mathbf{e}_k(\sin\alpha\mathbf{e}_y+\cos\alpha\mathbf{e}_x)}{\left(1-\frac{1}{c}\mathbf{e}_k\mathbf{v}_1\right)^2\left(1-\frac{1}{c}\mathbf{e}_k\mathbf{v}_2\right)^2}\right.$$
$$+\frac{1-(\mathbf{e}_k\mathbf{e}_z)^2+\frac{V^2}{c^2}\sin^2\psi\left(1-\left(\mathbf{e}_k(\sin\alpha\mathbf{e}_x+\cos\alpha\mathbf{e}_y)\right)^2\right)-2\frac{V}{c}\sin\psi\mathbf{e}_k(\sin\alpha\mathbf{e}_y-\cos\alpha\mathbf{e}_x)}{\left(1-\frac{1}{c}\mathbf{e}_k\mathbf{v}_3\right)^2\left(1-\frac{1}{c}\mathbf{e}_k\mathbf{v}_4\right)^2} \quad (6)$$
$$\left.-2\cos(2k_xx_0)\frac{1-(\mathbf{e}_k\mathbf{e}_z)^2+\frac{V^2}{c^2}\sin^2\psi\left(\sin^2\alpha\left(1-(\mathbf{e}_k\mathbf{e}_x)^2\right)-\cos^2\alpha\left(1-(\mathbf{e}_k\mathbf{e}_y)^2\right)\right)-2\frac{V}{c}\sin\psi\sin\alpha\mathbf{e}_k\mathbf{e}_y}{\left(1-\frac{1}{c}\mathbf{e}_k\mathbf{v}_1\right)\left(1-\frac{1}{c}\mathbf{e}_k\mathbf{v}_2\right)\left(1-\frac{1}{c}\mathbf{e}_k\mathbf{v}_3\right)\left(1-\frac{1}{c}\mathbf{e}_k\mathbf{v}_4\right)}\right\}.$$

RESULTS AND DISCUSSION

The characteristics of the resulting radiation are qualitatively determined by each of the four partial contributions in vector **I** (3) and the vector cross product $\mathbf{k}\times\mathbf{I}$ entering (2) of the four charges involved in generating radiation, as well as their interference. On the one hand, in the case of a relativistic particle ($v\to c$), the denominator of each of the four partial terms is small in the direction of **k** (the radiation direction), which is close to the direction of motion of the corresponding charge. On the other hand, the vector cross product of **k** with the corresponding term is small near this direction, approaching zero in the case of **k** parallel to the corresponding velocity. The combination of these two factors leads to the characteristic funnel-shaped angular dependence typical of transition radiation from relativistic particles (with a characteristic opening angle on the order of γ^{-1}, where $\gamma = (1 - v^2/c^2)^{-1/2}$ is the Lorentz factor of the particle) for each of the four partial contributions (Fig. 2). To illustrate the effect of the interference of partial contributions on the nature of the resulting radiation, we consider two specific cases.

First, let us consider the case where the trajectory of the incident particle lies in the plane (x, z), i.e., $\alpha = \pi$. The expressions for vector **I** and the spectral-angular radiation density are significantly simplified in this case since $\mathbf{v}_3 = -\mathbf{v}_2$ and $\mathbf{v}_4 = -\mathbf{v}_1$. The vector cross product $\mathbf{k}\times\mathbf{I}$ entering (2) is proportional to the amplitude of the magnetic field in the emitted wave, and the

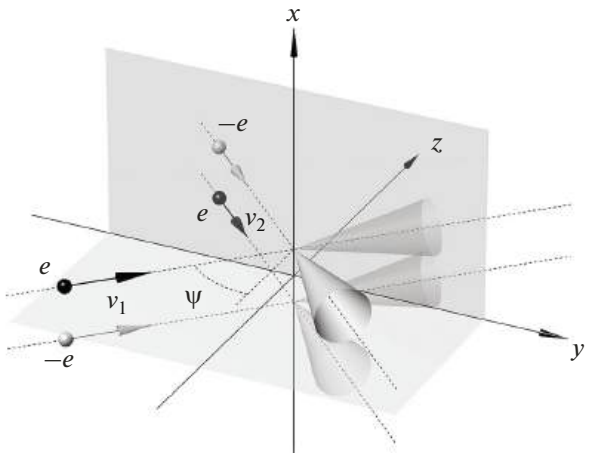

Fig. 2. Schematic representation of the four partial contributions to the radiation (from the incident particle and its three images) in the particular case of $\alpha = \pi/2$.

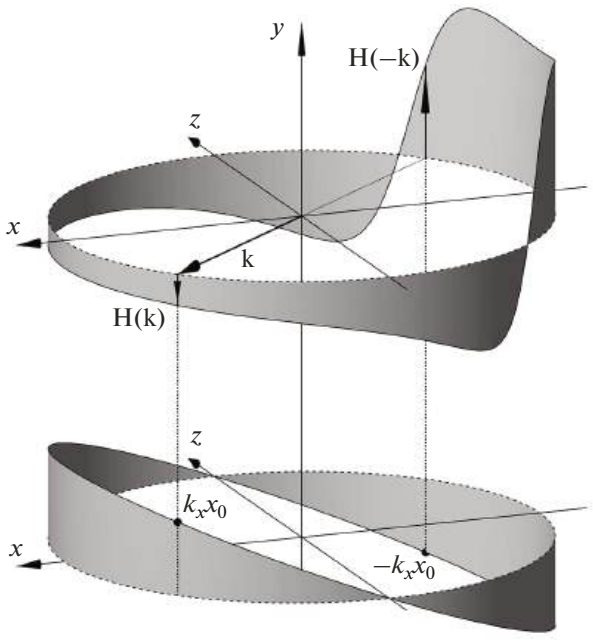

Fig. 3. (top) Contribution of the first term in (4) in the particular case of $\alpha = \pi$ to the amplitude of the magnetic field of waves emitted in the plane (x, z), and the contribution of the second term for a given **k**, i.e., the opposite point in the graph ($\mathbf{k}\to -\mathbf{k}$); (bottom) phase shifts of these two terms.

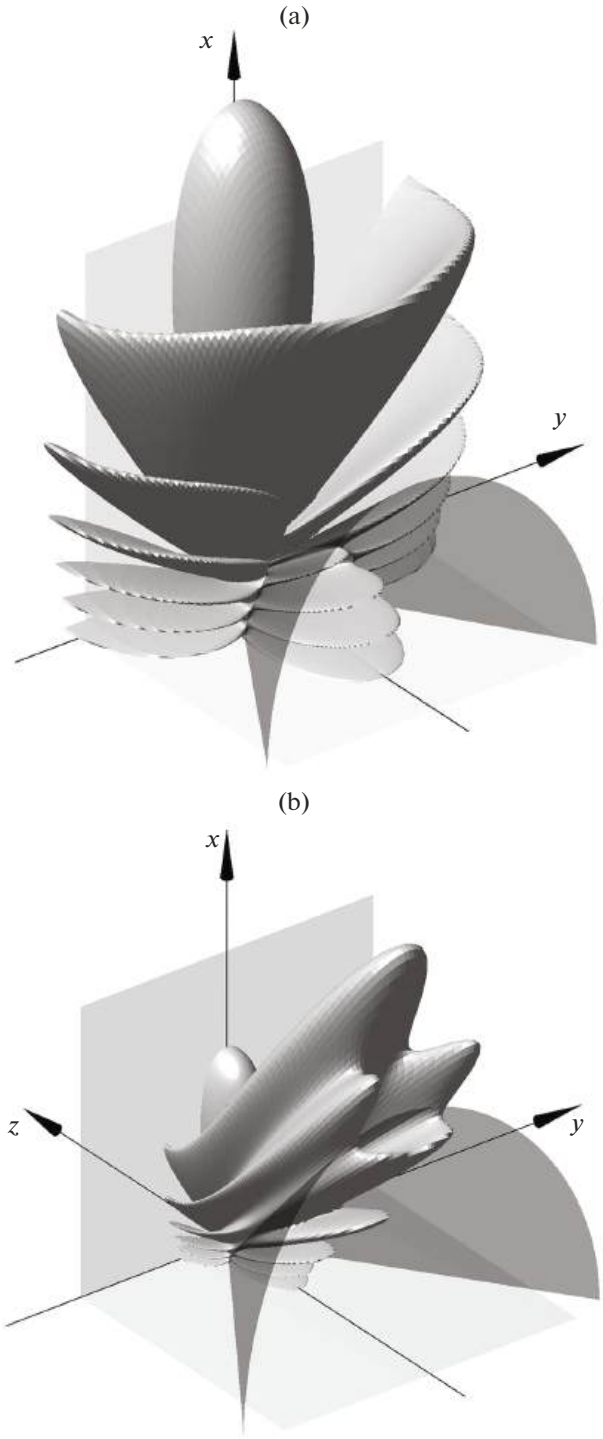

Fig. 4. Radiation pattern for $\psi = \pi/4$, $\alpha = \pi$, and $x_0\omega/c = 20$ according to (7) for the cases $v = (a)\ 0.9c$ and $(b)\ 0.99c$. The conical surface on both graphs indicates the directions of radiation where condition (8) is satisfied.

second pair of terms coincides with the first one with the replacement $\mathbf{k} \to -\mathbf{k}$. Figure 3 illustrates the radiation in the plane (x, z). Its upper part depicts the contribution to the amplitude of the magnetic field of the

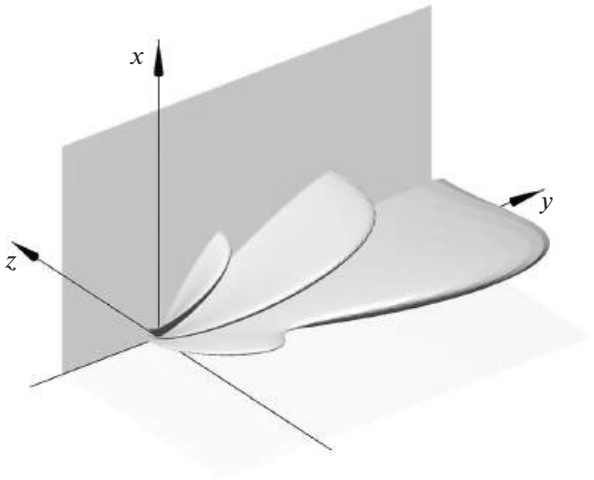

Fig. 5. Radiation pattern for $\psi = \pi/4$ and $\alpha = \pi/2$ according to (7) for the case of $v = 0.95c$, $x_0\omega/c = 10$.

emitted wave $\mathbf{H}(\mathbf{k})$ (resulting from substitution into the vector cross product $\mathbf{k} \times \mathbf{I}$ of the first term in (4) for different directions of the wave vector $\mathbf{k}$ (we recall that actual radiation occurs only in directions determined by the inequalities $k_x > 0$, $k_z < 0$) and simultaneously, according to the aforementioned, the contribution of the second term $\mathbf{H}(-\mathbf{k})$. The lower part of Fig. 3 illustrates the corresponding phase shifts associated with these two contributions.

The general equation for the spectral-angular radiation density (6) is simplified ($\alpha = \pi$) to

$$\frac{dE}{d\omega d\Omega} = \frac{e^2v^2}{\pi^2c^3}\cos^2\psi \times \left\{ \frac{\sin^2\theta + \frac{v^2}{c^2}\sin^2\psi\left(1 - \left(\mathbf{e}_k\mathbf{e}_y\right)^2\right) + 2\frac{v}{c}\sin\psi\mathbf{e}_k\mathbf{e}_x}{\left(1 - \frac{1}{c}\mathbf{e}_k\mathbf{v}_1\right)^2\left(1 - \frac{1}{c}\mathbf{e}_k\mathbf{v}_2\right)^2} \right.$$
$$+ \frac{\sin^2\theta + \frac{v^2}{c^2}\sin^2\psi\left(1 - \left(\mathbf{e}_k\mathbf{e}_y\right)^2\right) - 2\frac{v}{c}\sin\psi\mathbf{e}_k\mathbf{e}_x}{\left(1 + \frac{1}{c}\mathbf{e}_k\mathbf{v}_1\right)^2\left(1 + \frac{1}{c}\mathbf{e}_k\mathbf{v}_2\right)^2} \quad (7)$$
$$- 2\cos\left(2k_xx_0\right)$$
$$\left. \times \frac{\sin^2\theta - \frac{v^2}{c^2}\sin^2\psi\left(1 - \left(\mathbf{e}_k\mathbf{e}_y\right)^2\right)}{\left(1 - \frac{1}{c}\mathbf{e}_k\mathbf{v}_1\right)\left(1 - \frac{1}{c}\mathbf{e}_k\mathbf{v}_2\right)\left(1 + \frac{1}{c}\mathbf{e}_k\mathbf{v}_1\right)\left(1 + \frac{1}{c}\mathbf{e}_k\mathbf{v}_2\right)} \right\}.$$

The interference term becomes zero for radiation angles satisfying the condition

$$\sin^2\theta = \frac{\frac{v^2}{c^2}\sin^2\psi}{1 + \frac{v^2}{c^2}\sin^2\psi\sin^2\varphi}. \quad (8)$$

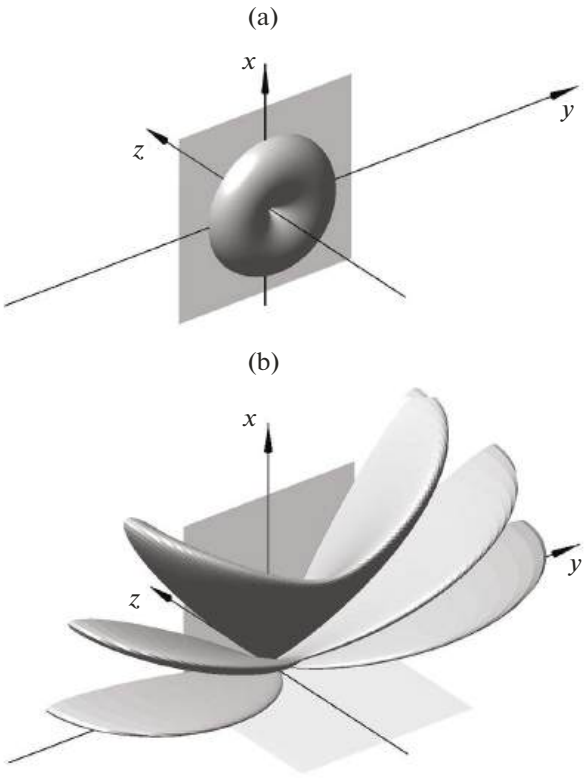

Fig. 6. Radiation pattern of a nonrelativistic particle (a) on a vertical plane and (b) considering the effect of a horizontal reflecting plane: $\psi = \pi/4$, $\alpha = \pi/2$, $v = 0.05c$, and $x_0\omega/c = 10$.

The signs of the second multiplier in the interference term on both sides of the surface defined by this condition (Fig. 4) are opposite. Meanwhile, the multiplier $\cos(2k_x x_0)$ in the interference term leads to the appearance of maxima and minima with the x axis as the axis of symmetry. All of this collectively forms a highly complex pattern of angular distribution of radiation.

Now, let us consider the case where the velocity of the incident particle is parallel to the plane (y, z), i.e., $\alpha = \pi/2$. The general equation (6) is simplified due to $\mathbf{v}_3 = \mathbf{v}_1$ and $\mathbf{v}_4 = \mathbf{v}_2$ (Fig. 2). The second multiplier in the interference term maintains its sign throughout the entire range of emission angles, so $\cos(2k_x x_0)$ remains the only sign-alternating multiplier in the interference term, leading to simplification of the interference pattern (Fig. 5).

The angular distribution appears most straightforward when the particle is nonrelativistic. As seen from (4) taking into account (5), in this case, the dependence of $\mathbf{I}$ on the direction of the incident particle velocity becomes negligibly small, and the direction of $\mathbf{I}$ becomes normal to the plane (x, y). Therefore, the angular distribution of transient radiation from a nonrelativistic particle on an infinite plane (described by the vector cross product of $\mathbf{k}$ and either the first or second term in Eq. (5)) is symmetric with respect to the normal to the metal surface, with zero intensity in this direction ([19] and Fig. 2a in [15]). Interference arising from the presence of two terms in (4) leads to the angular distribution shown in Fig. 6. The nature of the interference, determined solely by the term $\cos(2k_x x_0)$ in the case of nonrelativistic particles, is independent of the magnitude or direction of particle velocity. Therefore, counting the number of interference maxima on the radiation pattern at a given radiation frequency allows inference about the value of the coordinate x_0, which can be used for beam monitoring.

CONCLUSIONS

The study derived equations describing transition radiation on a conducting target in the form of two infinite half-planes intersecting at right angles. The description is based on the mirror-image method known from electrostatics. This approach yields a clear interpretation of the angular distribution of the resulting radiation, depending on the magnitude and direction of velocity of the incident particle, as well as the coordinates of the point of particle impact on the surface of the conductor, as a result of the interference of four partial contributions from the real charge and its three images in the radiation field.

The simplest interference occurs in two cases: when a relativistic particle is incident onto one half-plane parallel to the other half-plane (i.e., $\alpha = \pi/2$) and when a nonrelativistic particle impacts regardless of its velocity direction. In these scenarios, it appears feasible to extract information about the particle's impact point on the conductor from the interference pattern. This, in turn, could serve as the foundation for a new beam diagnostics method.

FUNDING

This work was funded by the institutional budget of Belgorod State National Research University. No additional grants to carry out or direct this particular research were obtained.

CONFLICT OF INTEREST

The authors of this work declare that they have no conflicts of interest.

REFERENCES

1. V. L. Ginzburg and V. N. Tsytovich, *Transition Radiation and Transition Scattering* (Adam Hilger, Bristol U.K., 1990).
2. J. D. Jackson, *Classical Electrodynamics* (John Wiley and Sons, 1962).
3. V. V. Batygin and I. N. Toptygin, *Collection of Problems on Electrodynamics* (Nauchno-Issled. Tsentr Regulyarn. Khaotich. Dinamika, Moscow, 2002) [in Russian].

4. I. Frank and V. Ginzburg, J. Phys. USSR **9** (5), 353 (1945).
5. N. F. Shul'ga, V. V. Syshchenko, and E. A. Larikova, Nucl. Instrum. Methods Phys. Res., Sect. B **402**, 167 (2017). https://doi.org/10.1016/j.nimb.2017.03.013
6. V. V. Syshchenko, E. A. Larikova, and Yu. P. Gladkih, JINST **12**, C12057 (2017). https://doi.org/10.1088/1748-0221/12/12/C12057
7. V. V. Syshchenko and E. A. Larikova, J. Surf. Invest.: X-ray, Synchrotron. Neutron. Tech. **13** (2), 359 (2019). https://doi.org/10.1134/S1027451019020393
8. N. F. Shul'ga and V. V. Syshchenko, Nucl. Instrum. Methods Phys. Res., Sect. B **452**, 55 (2019). https://doi.org/10.1016/j.nimb.2019.05.066
9. V. V. Syshchenko and E. A. Larikova, J. Surf. Invest.: X-ray, Synchrotron. Neutron. Tech. **13** (5), 990 (2019). https://doi.org/10.1134/S1027451019050367
10. L. Wartski, S. Roland, J. Lasalle, M. Bolore, and G. Filippi, J. Appl. Phys. **46**, 3644 (1975). https://doi.org/10.1063/1.322092
11. D. W. Rule, Nucl. Instrum. Methods Phys. Res., Sect. B **24/25**, 901 (1987). https://doi.org/10.1016/S0168-583X(87)80275-6
12. M. Castellano and V. A. Verzilov, Phys. Rev. Accel. Beams **1**, 062801 (1998). https://doi.org/10.1103/PhysRevSTAB.1.062801
13. A. P. Potylitsyn, *Electromagnetic Radiation of Electrons in Periodic Structures*, Vol. 243: *Springer Tracts in Modern Physics* (Springer, Berlin–Heidelberg, 2011). https://doi.org/10.1007/978-3-642-19248-7
14. R. Singh and T. Reichert, Phys. Rev. Accel. Beams **25**, 032801 (2022). https://doi.org/10.1103/PhysRevAccelBeams.25.032801
15. R. Singh, T. Reichert, and B. Walasek-Hoehne, Phys. Rev. Accel. Beams **25**, 072801 (2022). https://doi.org/10.1103/PhysRevAccelBeams.25.072801
16. I. I. Abbasov, B. M. Bolotovskii, and V. A. Davydov, Usp. Fiz. Nauk **149** (4), 709 (1986). https://doi.org/10.3367/UFNr.0149.198608f.0709
17. V. A. Bazylev and N. K. Zhevago, *Radiation of Fast Particles in Matter and in External Fields* (Nauka, Moscow, 1987) [in Russian].
18. A. I. Akhiezer and N. F. Shulga, *Electrodynamics of High Energies in Matter* (Nauka, Moscow, 1993) [in Russian].
19. V. V. Syshchenko and V. A. Krivtsov, Prikl. Matem. Fiz. **54** (4), 242 (2022). https://doi.org/10.52575/2687-0959-2022-54-4-242-251

Translated by O. Zhukova